Power Hardware-in-the-Loop Assessment of Co-located Battery Energy Storage for EV Charging Stations within Distribution Networks

Kwabena A. Kyeremeh, Steven B. Poore, and Dan M. Ionel
SPARK Laboratory, Stanley and Karen Pigman College of Engineering, University of Kentucky, Lexington, KY, USA
kwabena.kyeremeh@uky.edu, stevenpoore@uky.edu, dan.ionel@ieee.org

***Abstract*—High-power electric vehicle (EV) charging stations may introduce operational challenges in distribution networks by imposing concentrated, time-varying loads on infrastructure not designed for such demand patterns. This paper develops a voltage sensitivity-based control strategy for Battery Energy Storage Systems (BESS) co-located with EV charging stations to decrease grid impacts induced by EV charging. A Power Hardware-in-the-Loop (PHIL) testbed is developed to enable assessment of the proposed control approach under realistic operating conditions. Controller performance is evaluated through a simulation-in-the-loop case study conducted on the IEEE 8500-node distribution test feeder. The results demonstrate that the proposed strategy effectively maintains voltage regulation and reduces peak transformer loading by approximately 55% compared to the EV-only case. Experimental validation conducted using the developed testbed further confirms the effectiveness of the approach in regulating voltage and minimizing network loading under realistic operating conditions.**

***Index Terms*—Power Hardware-in-the-Loop (PHIL), Battery Energy Storage System, Electric Vehicle, Co-location, Grid Impact Assessment, Distribution Network, EV Charging Station**

I. Introduction

The electrification of the transportation sector, driven by the growing adoption of electric vehicles (EVs), may introduce significant operational challenges to distribution networks [1]–[3]. High-power EV charging stations, may impose substantial and highly variable loading conditions, resulting in voltage deviations, transformer overloading, and reduced power quality. These impacts are especially pronounced in low- and medium-voltage feeders with limited hosting capacity, where the temporal coincidence of EV charging demand with existing peak loads increases network stress [4], [5].

Battery Energy Storage Systems (BESS) may provide an effective solution for mitigating the impacts of EV charging on distribution networks. At the distribution level, BESS can provide multiple operational services, including peak shaving, voltage regulation, load leveling, and power quality support [6]. When co-located with EV charging infrastructure, BESS enables localized energy balancing by charging during low-demand periods and discharging during peak conditions, thereby reducing the net power demand observed by the upstream network and deferring infrastructure upgrades [7].

Conventional simulation approaches, including steady-state and offline electromagnetic transient (EMT) studies, are often insufficient to fully capture system behavior under realistic operating conditions, as they rely on simplified representations and may not accurately reflect the interactions between hardware, control systems, and network dynamics [8]. In contrast, Power Hardware-in-the-Loop (PHIL) simulation enables the integration of hardware with real-time digital simulation, allowing for high-fidelity validation of control strategies and system performance. A PHIL testbed provides a platform to evaluate the closed-loop behavior of co-located BESS and EV charging systems, including converter dynamics, interface delays, and measurement uncertainties [9], [10].

This paper presents a coordinated control strategy for co-located BESS and EV charging infrastructure to enhance voltage stability and enable peak shaving. A PHIL testbed, comprising a real-time microgrid test-bench, a power converter, and a programmable DC sink/source for EV charging emulation, is developed to experimentally validate the proposed control strategy. Software-in-the-Loop (SIL) simulation results demonstrating the effectiveness of the proposed controller are discussed. Results from an experimental validation of the approach in achieving voltage regulation and peak shaving under realistic operating conditions are also analyzed.

II. Design and Implementation of a PHIL-Based EV Charging Testbed Incorporating a co-located Battery Energy Storage System

A power hardware-in-the-loop testbed is developed, as shown in Fig. 1, to experimentally assess distribution-level impacts of EV charging and validate a sensitivity-based predictive voltage control strategy for a co-located BESS under real-time closed-loop operation. The platform is implemented on an OPAL-RT OP1420 microgrid testbench, incorporating two 5kW four-quadrant power amplifiers to enforce point-of-common-coupling (PCC) voltage conditions and facilitate power exchange between simulated and physical subsystems. The microgrid testbench is interfaced with OPAL-RT's OP5707XG real-time simulator through an SFP fiber optic cable for high-speed, low-latency data communication and real-time signal exchange between the simulator and the hardware components in the Hardware-in-the-Loop (HIL) setup.

Charging behavior of the EV is emulated through a power converter interfaced with a programmable bidirectional DC power supply/sink, which allows flexible modeling of various charging profiles and supports bidirectional DC power transfer

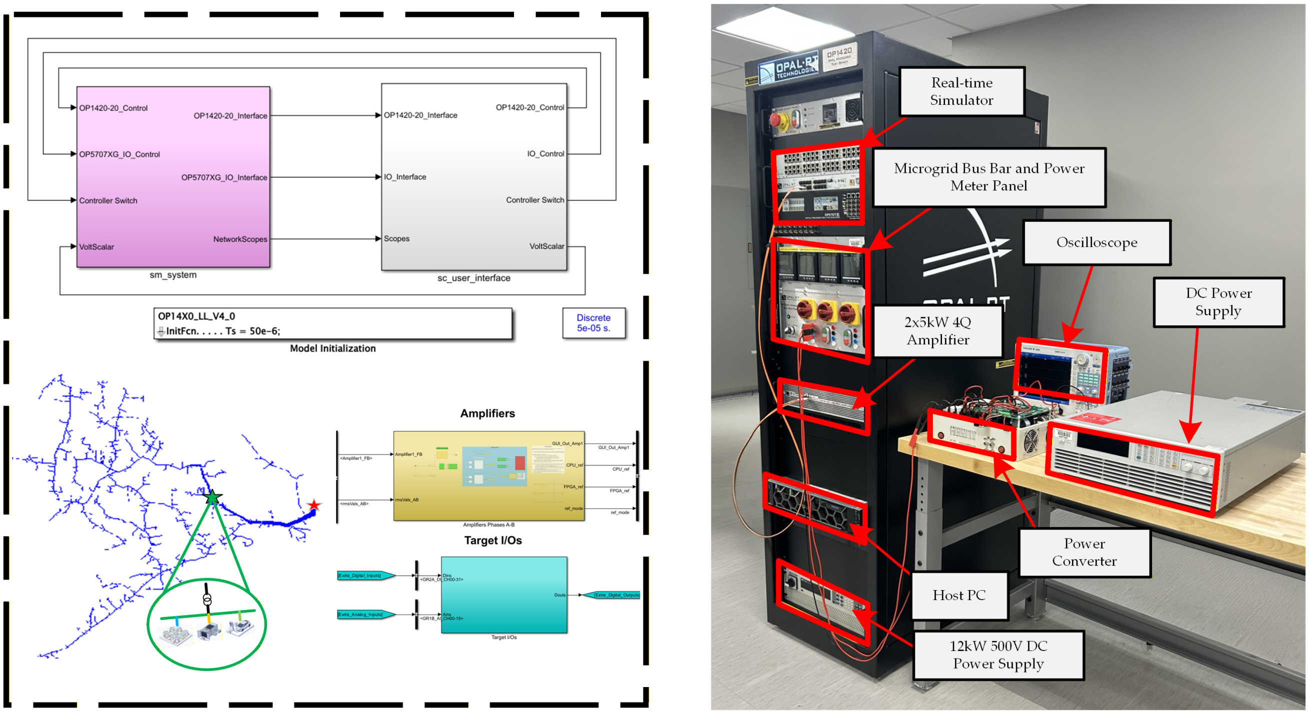

(a) (b)

Fig. 1. Real-time Power Hardware-in-the-Loop testbed for EV impact assessment on distribution networks with OPAL-RT simulation model depicting the distribution network topology and controller interfaces (a), and laboratory hardware platform including real-time simulator, power amplifiers, power converter, and DC power supplies for emulating EV charging dynamics (b).

capability. The distribution network model is implemented in a MATLAB/Simulink environment and executed within OPAL-RT's RT-Lab by the real-time simulator.

III. Voltage Sensitivity-based Control algorithm for co-located BESS with EV charging Station

A control strategy is proposed to reduce the impact of EV charging stations on bus voltages and transformer loading of distribution networks. The control scheme is based on voltage sensitivity analysis to dispatch a BESS, which is electrically co-located with an EV charging station. The controller is implemented within the real-time simulation framework and interfaced with the PHIL platform integrated with an emulated EV charging station.

At the point of interconnection (POI) of the electrically co-located EV charging station and BESS, the net active power observed by the upstream feeder is given by:

$$P_{\text{net}}(k) = P_{\text{EV}}(k) + P_{\text{L}}(k) - P_{\text{B}}(k), \tag{1}$$

where $P_{\text{EV}}(k)$ and $P_{\text{L}}(k)$ denote the aggregate EV charging demand and local base load at time step k, respectively. The BESS power, $P_{\text{B}}(k)$, follows the convention $P_{\text{B}}(k) > 0$ for discharging (grid support) and $P_{\text{B}}(k) < 0$ for charging.

The proposed control strategy exploits the local voltage–power sensitivity at the point of common coupling (PCC), defined as:

$$S_v(k) = \frac{\partial V_{\text{pcc}}(k)}{\partial P}, \tag{2}$$

which characterizes the incremental voltage response to variations in active power injection. As outlined in Algorithm 1, $S_v(k)$ is obtained using a perturbation-based estimation approach and periodically updated to capture time-varying feeder conditions. At each time step, the controller predicts the PCC voltage using a first-order approximation:

$$\hat{V}_{\text{pcc}}(k+1) = V_{\text{pcc}}(k) + S_v(k)\big(-P_{\text{B}}(k)\big). \tag{3}$$

To ensure acceptable operation, the predicted voltage is constrained as

$$V_{\min} \leq \hat{V}_{\text{pcc}}(k+1) \leq V_{\max}, \tag{4}$$

which yields the voltage-feasible BESS operating region:

$$\frac{V_{\text{pcc}}(k) - V_{\max}}{S_v(k)} \leq -P_{\text{B}}(k) \leq \frac{V_{\text{pcc}}(k) - V_{\min}}{S_v(k)}. \tag{5}$$

In addition to voltage regulation, the controller incorporates load-driven objectives for peak shaving and valley charging based on the net uncontrolled demand;

$$P_{\text{unc}}(k) = P_{\text{EV}}(k) + P_{\text{L}}(k), \tag{6}$$

thereby enabling coordinated voltage support and demand shaping. The final BESS dispatch is determined by combining the voltage-feasible region with physical and operational constraints, including converter power limits, state-of-charge (SoC) bounds, and ramp-rate limits. The commanded power

Algorithm 1 Voltage-sensitivity-based control algorithm for co-located BESS with an EV charging station

Require: $V_{\text{bus}}, P_{\text{base}}, P_{\text{EV}}, \text{SoC}, P_{\text{prev}}$
Ensure: $P_{\text{net}}, P_{\text{BESS}}, \text{SoC}^{+}, e_V$

$V_{\text{pu}} \leftarrow V_{\text{bus}}/V_{\text{nom}}, \quad e_V \leftarrow V_{\text{ref}} - V_{\text{pu}}, \quad P_{\text{unc}} \leftarrow P_{\text{base}} + P_{\text{EV}}$
$P_{\text{dis}} \leftarrow \max\big(0, (\text{SoC} - \text{SoC}_{\text{min}})E_{\text{nom}}/\Delta t\big), \quad P_{\text{chg}} \leftarrow \max\big(0, (\text{SoC}_{\text{max}} - \text{SoC})E_{\text{nom}}/\Delta t\big)$
$P_{\text{min}}^{\text{phys}} \leftarrow \max(P_{\text{min}}^{\text{hw}}, -P_{\text{chg}}), \quad P_{\text{max}}^{\text{phys}} \leftarrow \min(P_{\text{max}}^{\text{hw}}, P_{\text{dis}})$
$P_{\text{min}}^{V} \leftarrow -(V_{\text{low}} - V_{\text{pu}})/S_{VP}, \quad P_{\text{max}}^{V} \leftarrow -(V_{\text{high}} - V_{\text{pu}})/S_{VP}$
$P_{\text{min}} \leftarrow \max(P_{\text{min}}^{\text{phys}}, P_{\text{min}}^{V}), \quad P_{\text{max}} \leftarrow \min(P_{\text{max}}^{\text{phys}}, P_{\text{max}}^{V})$
if $P_{\text{min}} > P_{\text{max}}$ **then**
  $P_{\text{min}} \leftarrow P_{\text{min}}^{\text{phys}}, \quad P_{\text{max}} \leftarrow P_{\text{max}}^{\text{phys}}$
end if
$P_{\text{raw}} \leftarrow \mathbf{1}_{V_{\text{pu}}<V_{\text{low}}} \frac{V_{\text{low}}-V_{\text{pu}}}{|S_{VP}|} - \mathbf{1}_{V_{\text{pu}}>V_{\text{high}}} \frac{V_{\text{pu}}-V_{\text{high}}}{|S_{VP}|} + \mathbf{1}_{P_{\text{unc}}>P_{\text{pk}}}(P_{\text{unc}} - P_{\text{pk}}) - \mathbf{1}_{P_{\text{unc}}<P_{\text{st}}}(P_{\text{st}} - P_{\text{unc}})$
$P_{\text{r}} \leftarrow \text{clip}\big(P_{\text{raw}}, [P_{\text{prev}} - \Delta P_{\text{max}}, \; P_{\text{prev}} + \Delta P_{\text{max}}]\big)$
$P_{\text{BESS}} \leftarrow \text{clip}\big(P_{\text{r}}, [P_{\text{min}}, P_{\text{max}}]\big)$
$P_{\text{net}} \leftarrow P_{\text{unc}} - P_{\text{BESS}}$
if $P_{\text{net}} > P_{\text{limit}}$ **then**
  $P_{\text{BESS}} \leftarrow \min(P_{\text{unc}} - P_{\text{limit}}, P_{\text{max}}^{\text{phys}}), \quad P_{\text{net}} \leftarrow P_{\text{unc}} - P_{\text{BESS}}$
end if
$\text{SoC}^{+} \leftarrow \text{sat}(\text{SoC} - P_{\text{BESS}}\Delta t/E_{\text{nom}}), \quad P_{\text{prev}} \leftarrow P_{\text{BESS}}$
return $P_{\text{net}}, P_{\text{BESS}}, \text{SoC}^{+}, e_V$

is thus obtained as:

$$P_{\text{B}}(k) = \text{clip}(P_{\text{r}}(k), \, [P_{\text{min}}(k), P_{\text{max}}(k)]) \,, \tag{7}$$

where $P_{\text{r}}(k)$ denotes the ramp-limited control action and $[P_{\text{min}}(k), P_{\text{max}}(k)]$ represents the intersection of voltage and SoC-constrained feasible regions. Finally, the feeder loading constraint is enforced by limiting the net power as:

$$P_{\text{net}}(k) \le P_{\text{limit}}, \tag{8}$$

which may override the BESS dispatch under heavily loaded conditions. The SoC dynamics are updated as:

$$\text{SoC}(k+1) = \text{SoC}(k) - \frac{P_{\text{B}}(k)\Delta t}{E_{\text{nom}}}, \tag{9}$$

ensuring operation within allowable energy limits.

IV. Coordinated BESS Control for Mitigating Grid Impacts of EV Charging

A case study of the proposed control strategy is conducted using a Simulation-in-the-Loop framework. The study is performed on a single-phase bus of the IEEE 8500-node test feeder in the phasor domain, where a 50kW EV charging station is co-located with a BESS and supplied through a 100kVA distribution transformer. A 6-hour analysis window from 16:00 to 22:00 is selected to capture periods of elevated residential baseload and frequent EV charging activity, representing a worst-case operating scenario for the distribution network. The base load and voltage profiles at the selected bus, in the absence of EV charging and BESS, are shown in Fig. 2 and serve as a benchmark case.

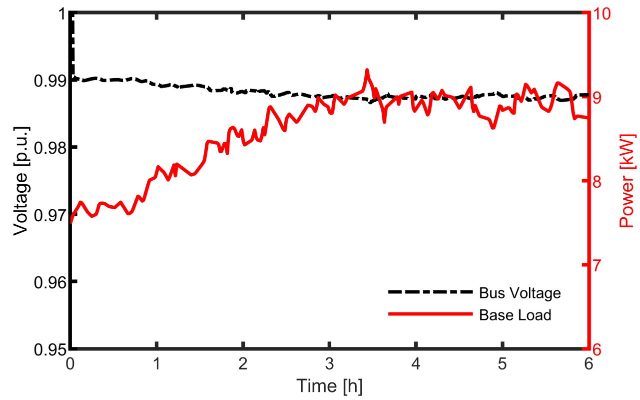

Fig. 2. Baseline operating condition of the study feeder without EV charging or BESS support over the study window. The results capture the inherent load-driven voltage variation of the feeder and establish a benchmark for EV charging and BESS integration evaluation.

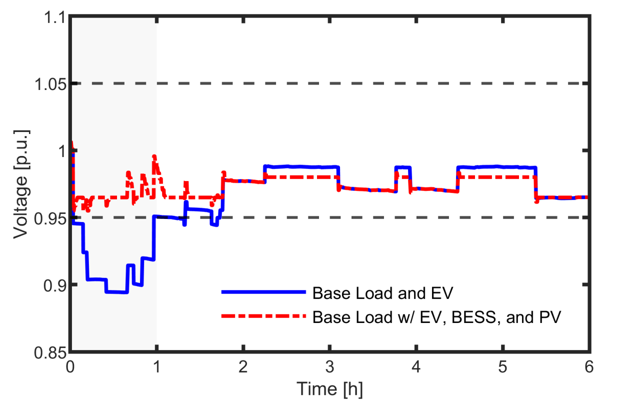

Fig. 3. Per-unit voltage response at the selected bus shows that EV charging alone leads to significant voltage drops below acceptable limits, whereas coordinated BESS operation effectively regulates voltage deviations and maintains bus voltage within operational limits.

The per-unit voltage response at the selected feeder bus under two operating conditions is presented in Fig. 3, both of which include the same underlying time-varying baseload. In the EV-only case, high-power charging results in voltage deviations that approach and periodically violate the ANSI C84.1 acceptable limits [11], reaching 0.89 p.u. and indicating inadequate voltage regulation under high loading conditions.

With the proposed coordinated BESS control strategy, the bus voltage is effectively regulated and maintained within acceptable operational limits throughout the evaluation period, with a 0.96p.u. minimum voltage. These results demonstrate that the proposed control strategy provides effective and reliable local voltage support, preserving adequate voltage margins under realistic loading conditions.

The impact of coordinated BESS operation on transformer loading is illustrated in Fig. 4. The shaded interval denotes the peak demand period, during which BESS dispatch reduces

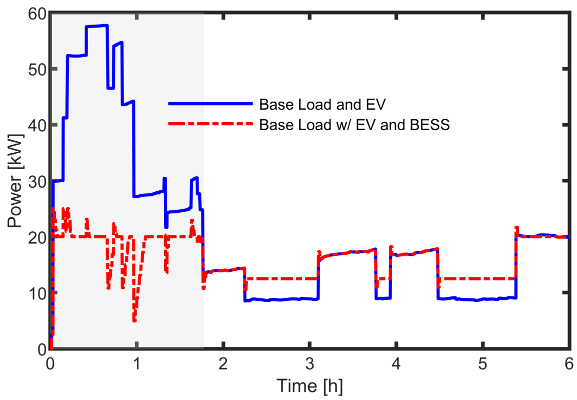

Fig. 4. Transformer loading profile under EV charging conditions with and without BESS support. The results demonstrate that the BESS effectively reduces peak transformer loading and smooths load variability over the 6-h operating period.

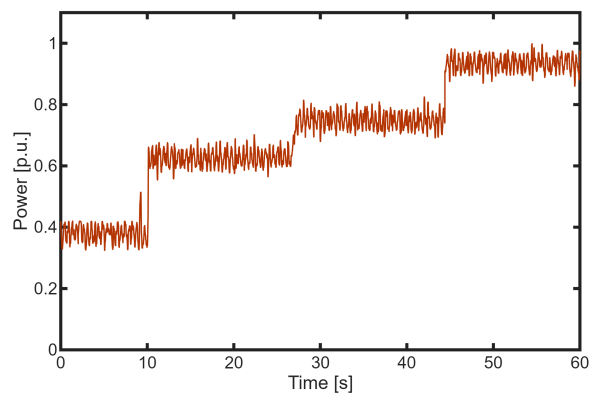

Fig. 6. Emulated EV step power demand profile recorded during PHIL testing over a 60-second window, used to assess the dynamic response of a co-located BESS under varying EV charging demand levels on the distribution network.

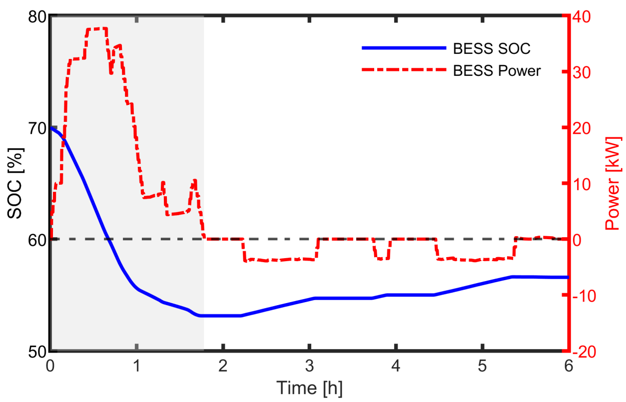

Fig. 5. State-of-charge and power dispatch profile of the BESS during the EV charging scenario. The shaded interval indicates peak-shaving operation, during which the BESS provides discharge support followed by controlled charging, maintaining SOC limits while mitigating EV-induced load peaks.

transformer loading by approximately 55% relative to the EV-only case, demonstrating the controller's effectiveness in limiting thermal stress through constraint-aware operation.

The corresponding BESS operating trajectory, including power dispatch and SOC profiles are shown in Fig. 5. During peak EV demand, the BESS discharges to support the feeder, followed by a transition to controlled charging once loading reduces, while maintaining the SOC within manufacturer-specified limits. This coordinated behavior enables sustained load and voltage regulation over the study period.

V. Implementation of a PHIL-based Control Strategy

To validate the proposed algorithm under realistic operating conditions, experimental testing is conducted using the developed PHIL testbed in real-time. The test system is based on a modified IEEE 13-bus distribution network, where a BESS and the emulated EV charging load are electrically co-located on a common bus. The EV charging demand follows a step-increase profile (Fig. 6), reflecting the abrupt load changes typical of EV charging events at the point of interconnection (POI). The experimental evaluation is carried out over a 60-second observation window, providing sufficient resolution to assess the dynamic response of the algorithm under the imposed disturbance.

The instantaneous voltage recorded at the POI under the combined effect of the EV charging and base load demands, in the absence of a controlled co-located BESS, is presented in Fig. 7(a). The results demonstrate persistent voltage limit violations throughout the observation window. In contrast, Fig. 7(b) illustrates the voltage profile obtained when the co-located BESS operates under the proposed control strategy, wherein the voltage is consistently maintained within the permissible operating bounds. The insets provide an enlarged view of the dynamic response over the interval between 56 s and 56.25 s, corresponding to the period of maximum EV charging demand, highlighting the transient behavior of both cases under peak loading conditions.

To further quantify the impact on voltage regulation, the average RMS voltage response as a function of the induced EV charging demand is presented in Fig. 8. Under light loading conditions, at approximately 0.4 pu active power, both the controlled and uncontrolled cases exhibit a comparable per-unit voltage of approximately 0.975 pu. As the load increases by about 50%, a divergence between the two cases begins to emerge, with the controlled case sustaining a voltage of 0.965 pu compared to 0.960 pu in the uncontrolled case. Upon approaching full loading at 1 pu, the uncontrolled voltage experiences a sharp deterioration, dropping to approximately 0.94 pu, which falls below the permissible operating limit. This behavior is effectively mitigated in the BESS-controlled scenario, where the proposed strategy successfully regulates the bus voltage within the acceptable range throughout the entire loading profile, demonstrating its efficacy in mitigating EV-induced voltage violations.

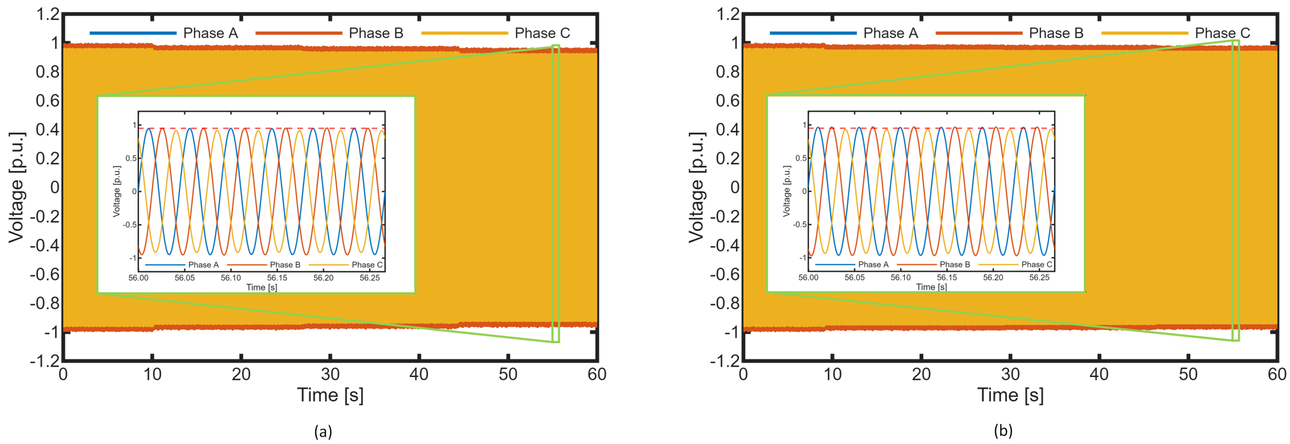

Fig. 7. Three-phase voltage magnitude (p.u.) at the point of interconnection: (a) the uncontrolled case and (b) with co-located BESS controller. The uncontrolled scenario exhibits voltage violations below the minimum allowable threshold, while the BESS controller effectively regulates voltages within acceptable limits. Insets present an exploded view of the corresponding steady-state sinusoidal waveforms.

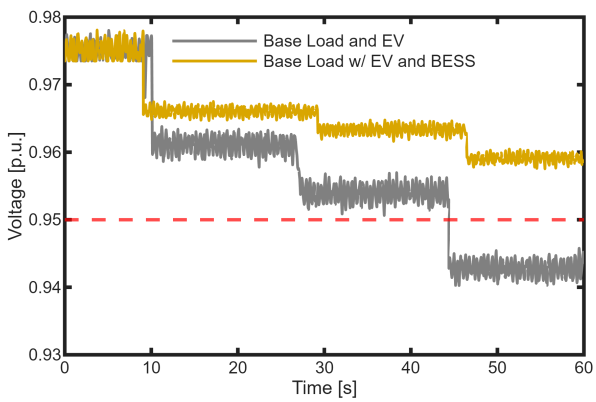

Fig. 8. Distribution network RMS voltage response (p.u.) under stepped EV power injection during PHIL testing is illustrated. The proposed BESS control strategy maintains voltage above the 0.95 p.u. regulatory limit (red dashed), demonstrating its effectiveness in mitigating EV-induced voltage violations.

VI. Conclusion

This paper presents a voltage sensitivity-based control strategy for battery energy storage systems and develops a Power Hardware-in-the-Loop testbed for its experimental evaluation. A assessment of the proposed approach is conducted through a simulation-in-the-loop analysis on a modified IEEE 8500-node distribution feeder under high-power EV charging conditions. Simulation results demonstrate that the proposed controller effectively regulates bus voltage within operational limits while simultaneously mitigating peak loading via constraint enforcement. Experimental laboratory validation of the proposed control algorithm conducted with the developed PHIL testbed, show that controlled co-located BESS effectively mitigates voltage deviations induced by EV charging.

Acknowledgment

The support of the University of Kentucky L. Stanley Pigman Chair in Power endowment is gratefully acknowledged. Any findings and conclusions expressed herein are those of the authors and do not necessarily reflect the views of the sponsor organization.

References

[1] R. E. Alden, A. Timilsina, S. Silvestri, and D. M. Ionel, "V2G Optimization for Dispatchable Residential Load Operation and Minimal Utility Cost," in *IEEE Transportation Electrification Conference Expo*, 2023.

[2] G. Benedetto, E. Bompard, A. Mazza, E. Pons, R. Jaboeuf, P. Tosco, and M. Zampolli, "Impact of bidirectional ev charging stations on a distribution network: a power hardware-in-the-loop implementation," *Sustainable Energy, Grids and Networks*, vol. 35, p. 101106, 2023.

[3] E. Ucer and M. J. Kisacikoglu, "Development of a hardware-in-the-loop testbed for a decentralized, data-driven electric vehicle charging control algorithm," *IEEE Transactions on Industry Applications*, vol. 60, no. 4, pp. 6622–6633, 2024.

[4] P. Roy, R. Ilka, J. He, Y. Liao, A. M. Cramer, J. Mccann, S. Delay, S. Coley, M. Geraghty, and S. Dahal, "Impact of Electric Vehicle Charging on Power Distribution Systems: A Case Study of the Grid in Western Kentucky," *IEEE Access*, vol. 11, pp. 49 002–49 023, 2023.

[5] M. H. Mobarak and J. Bauman, "Vehicle-Directed Smart Charging Strategies to Mitigate the Effect of Long-Range EV Charging on Distribution Transformer Aging," *IEEE Transactions on Transportation Electrification*, vol. 5, no. 4, pp. 1097–1111, 2019.

[6] K. A. Kyeremeh, G. M. Fischer, D. D. Lewis, A. Patrick, and D. M. Ionel, "Degradation Minimization of Utility-Scale Li-ion BESS Through Operational Optimization Employing an Equivalent Circuit Model," in *IEEE Energy Conversion Conference Congress and Exposition*, 2025.

[7] A. U. Rehman, J. Lu, B. Du, F. Bai, and M. J. Sanjari, "Efficient management of electric vehicle charging stations: Balancing user preferences and grid demands with energy storage systems and renewable energy," *Applied Energy*, vol. 393, p. 126147, 2025.

[8] Y. Wu, S. Duan, and L. Yang, "Optimization of Active Distribution Network for Electric Vehicle Charging–Swapping–Storage Integrated Station Considering Time-of-Use Pricing," *IEEE Transactions on Transportation Electrification*, vol. 12, no. 2, pp. 3267–3279, 2026.

[9] L. De Herdt, A. Shekhar, Y. Yu, G. R. C. Mouli, J. Dong, and P. Bauer, "Power Hardware-in-the-Loop Demonstrator for Electric Vehicle Charging in Distribution Grids," in *2021 IEEE Transportation Electrification Conference Expo (ITEC)*, 2021, pp. 679–683.

[10] M. Hosseinzadehtaher, D. Tiwari, N. Kouchakipour, A. Momeni, M. Lelic, and Z. Wu, "Grid Resilience Assessment during Extreme Fast Charging of Electric Vehicles via Developed Power Hardware-in-the-Loop," in *IEEE/AIAA Transportation Electrification Conference and Electric Aircraft Technologies Symposium*, 2022.

[11] *ANSI C84.1-2020: American National Standard for Electric Power Systems and Equipment—Voltage Ratings (60 Hz)*, American National Standards Institute Std. ANSI C84.1-2020, 2020.